

SUPPLEMENTAL INFORMATION FOR
Elucidating the impact of metal doping in $\text{Li}_{1.15}(\text{Ni}_{0.35}\text{Mn}_{0.65})_{0.85}\text{O}_2$ cathodes using high-throughput experiments and machine learning

Alex Hebert^{1,†}, Nooshin Zeinali Galabi^{1,†}, Michael Sieffert¹, Maxime Blangero^{2,*}, Eric McCalla^{1,*}
McGill University

1. Department of Chemistry, McGill University, Montreal, QC, Canada, H3A 0B8
2. Umicore Battery Materials Korea, 71, 3 Gongdan 2-Ro, Seobuk-Gu, CheonAn 331-200 Chungnam, South-Korea

[†] Contributed equally.

* Corresponding authors: maxime.blangero@ap.uminco.com and eric.mccalla@mcgill.ca

Table S1. Average atomic ratios of undoped materials at various sintering temperatures determined by ICP-OES. They are normalized such that $\text{Li}+\text{Ni}+\text{Mn}=2$ as in the target stoichiometry.

Sintering Temperature (°C)	Li	Mn	Ni
800	1.16	0.54	0.30
850	1.18	0.51	0.31
900	1.15	0.53	0.32

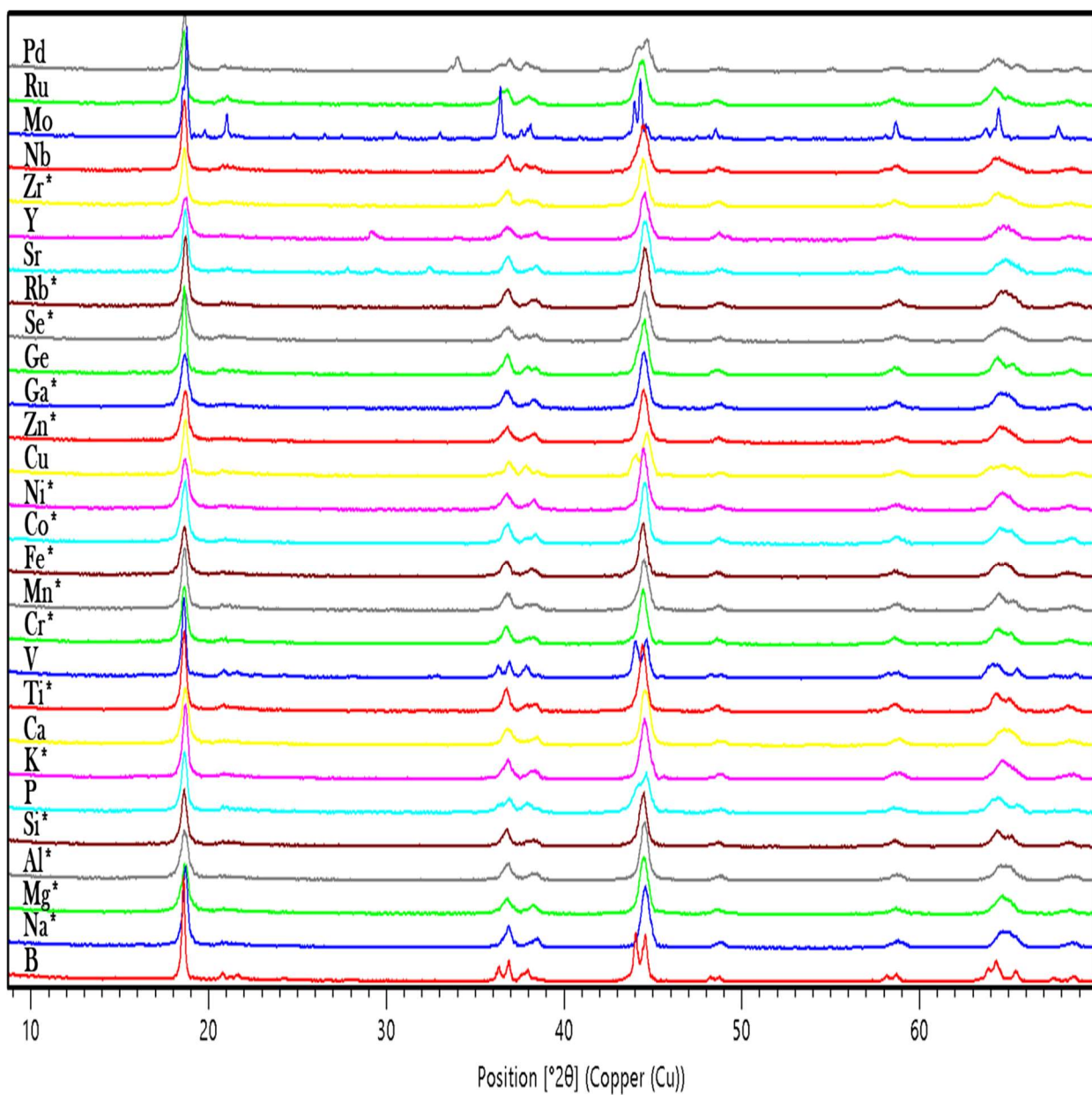


Figure S1. A and B show the XRD spectra of $\text{Li}_{1.15}(\text{Mn}_{0.65}\text{Ni}_{0.35})_{0.8}\text{M}_{0.05}\text{O}_2$; M=dopant, sintered at 800°C. Asterisks (*) indicate the single-phase materials.

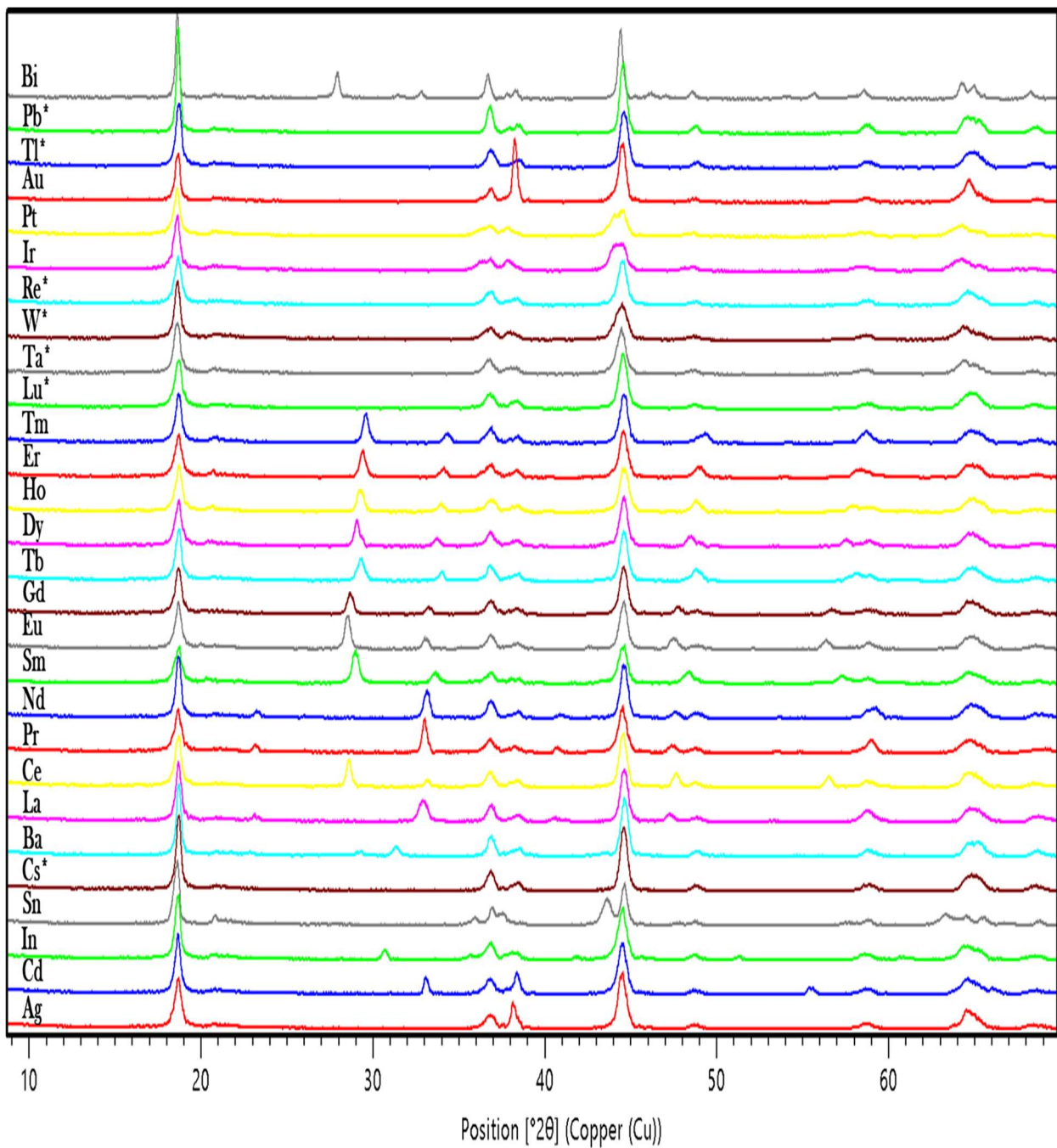


Figure S1 (continued).

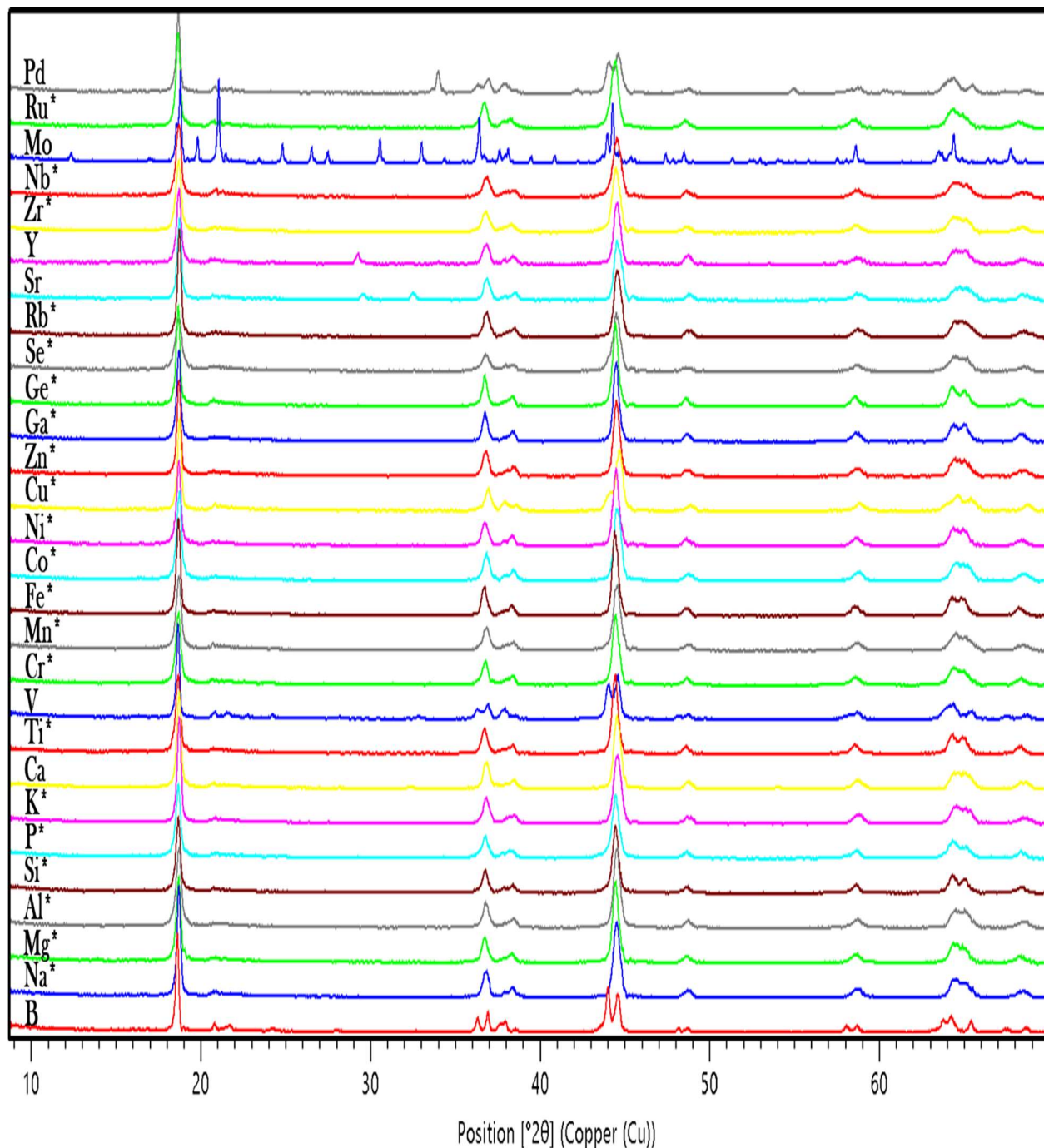


Figure S2. XRD spectra of $\text{Li}_{1.15}(\text{Mn}_{0.65}\text{Ni}_{0.35})_{0.8}\text{M}_{0.05}\text{O}_2$; M=dopant, sintered at 850°C . Asterisks (*) indicate the single-phase materials.

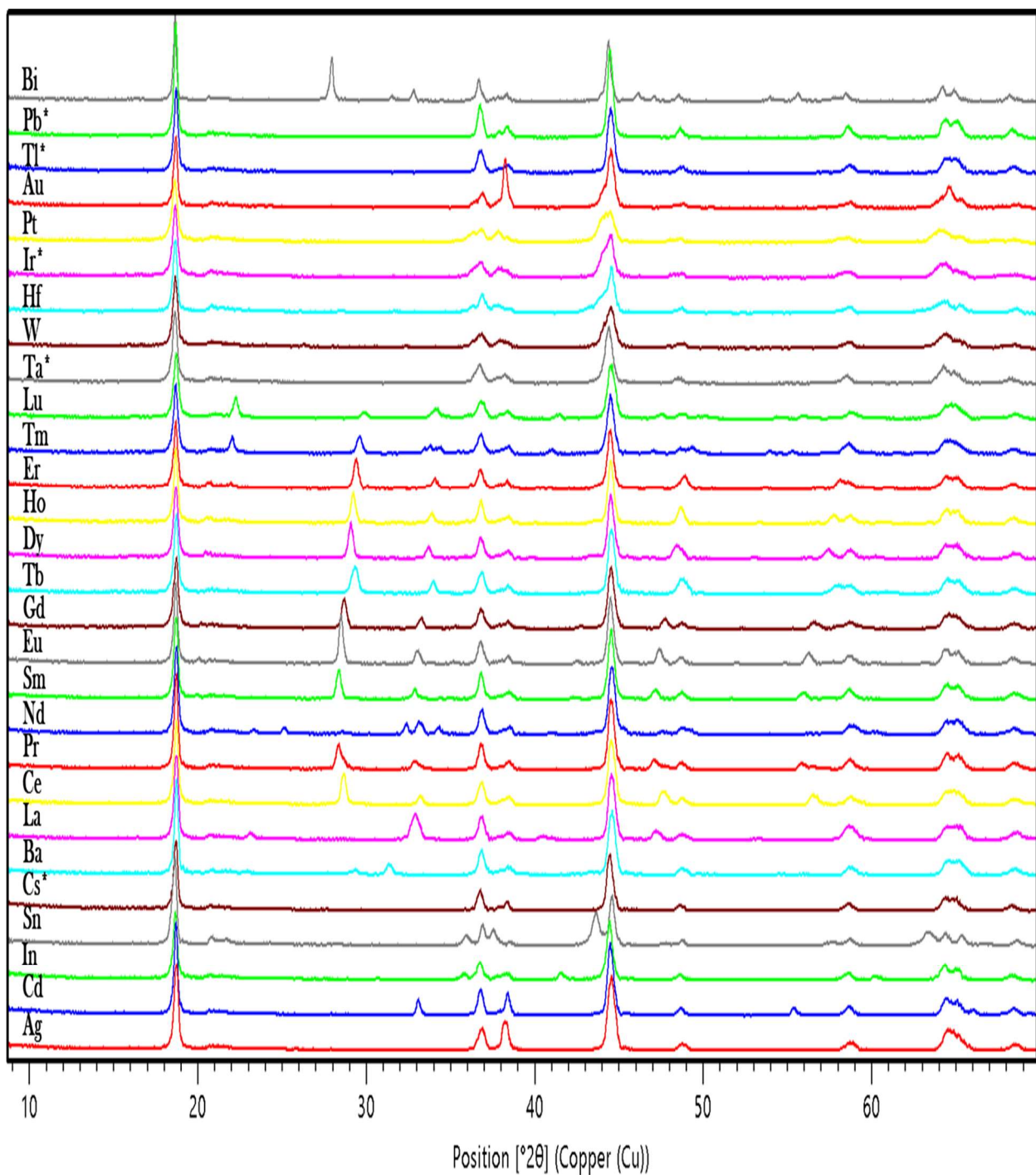


Figure S2 (continued).

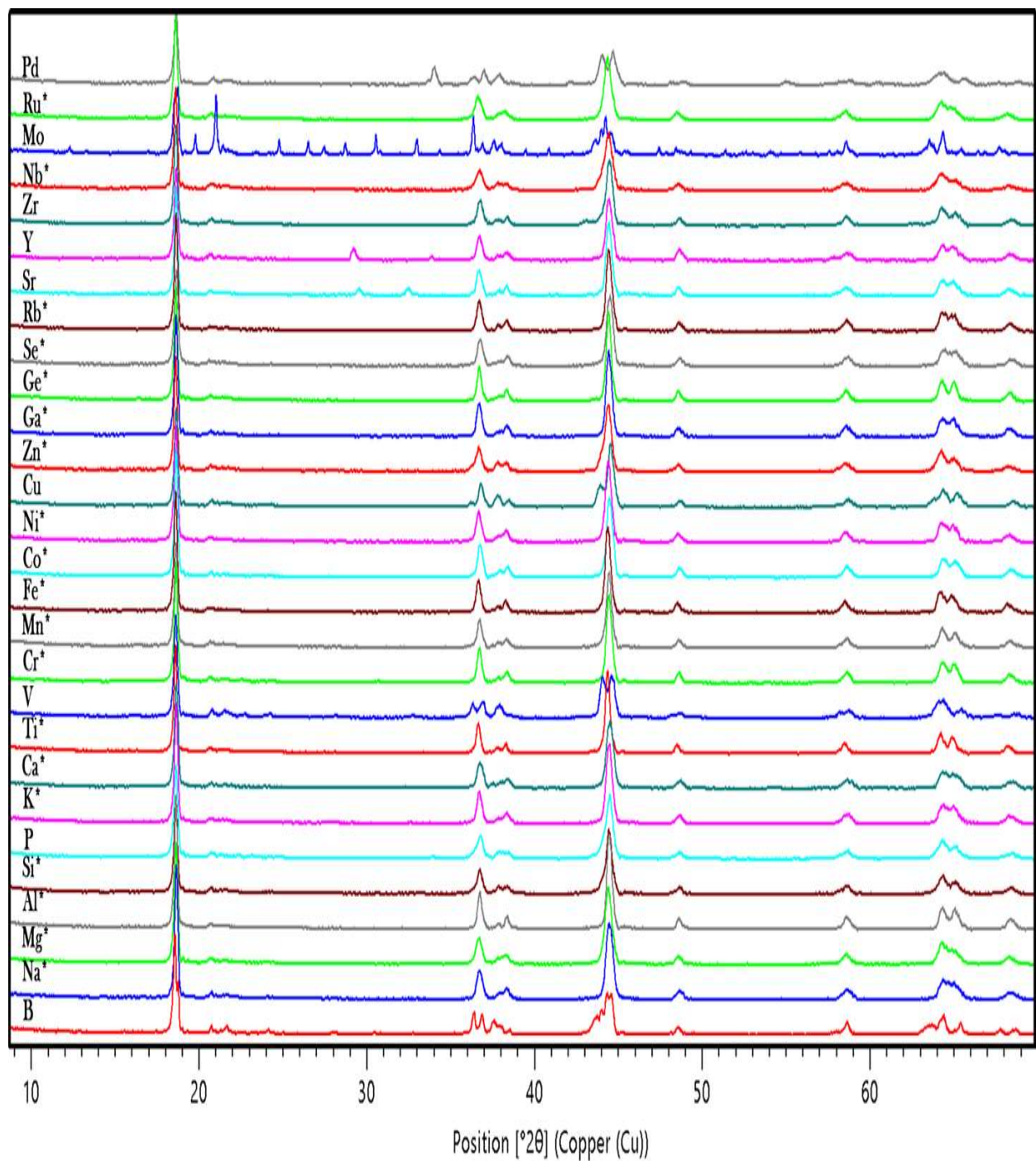


Figure S3. XRD spectra of $\text{Li}_{1.15}(\text{Mn}_{0.65}\text{Ni}_{0.35})_{0.8}\text{M}_{0.05}\text{O}_2$; M=dopant, sintered at 900 °C. Asterisks (*) indicate the single-phase materials.

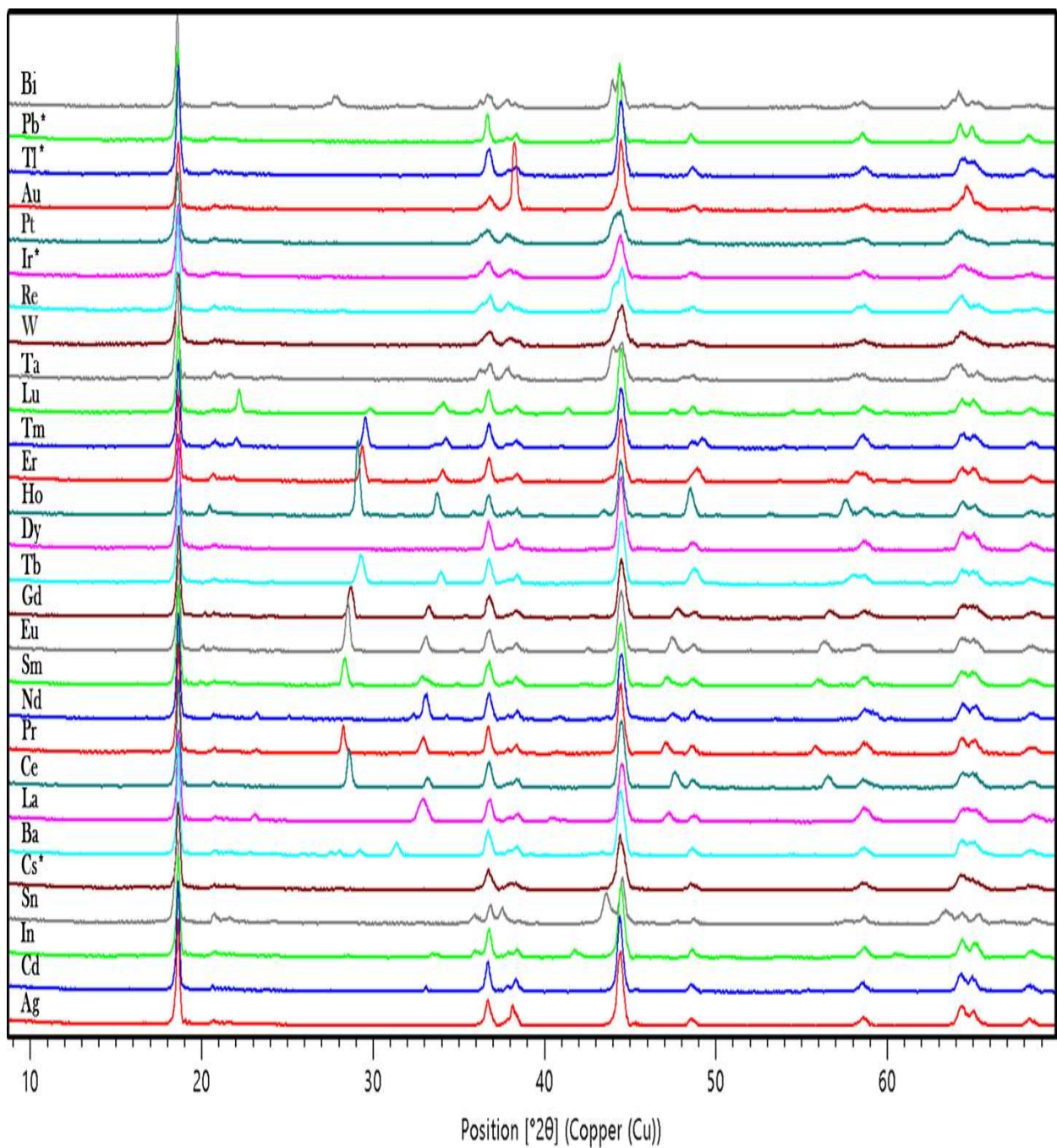


Figure S3 (continued).

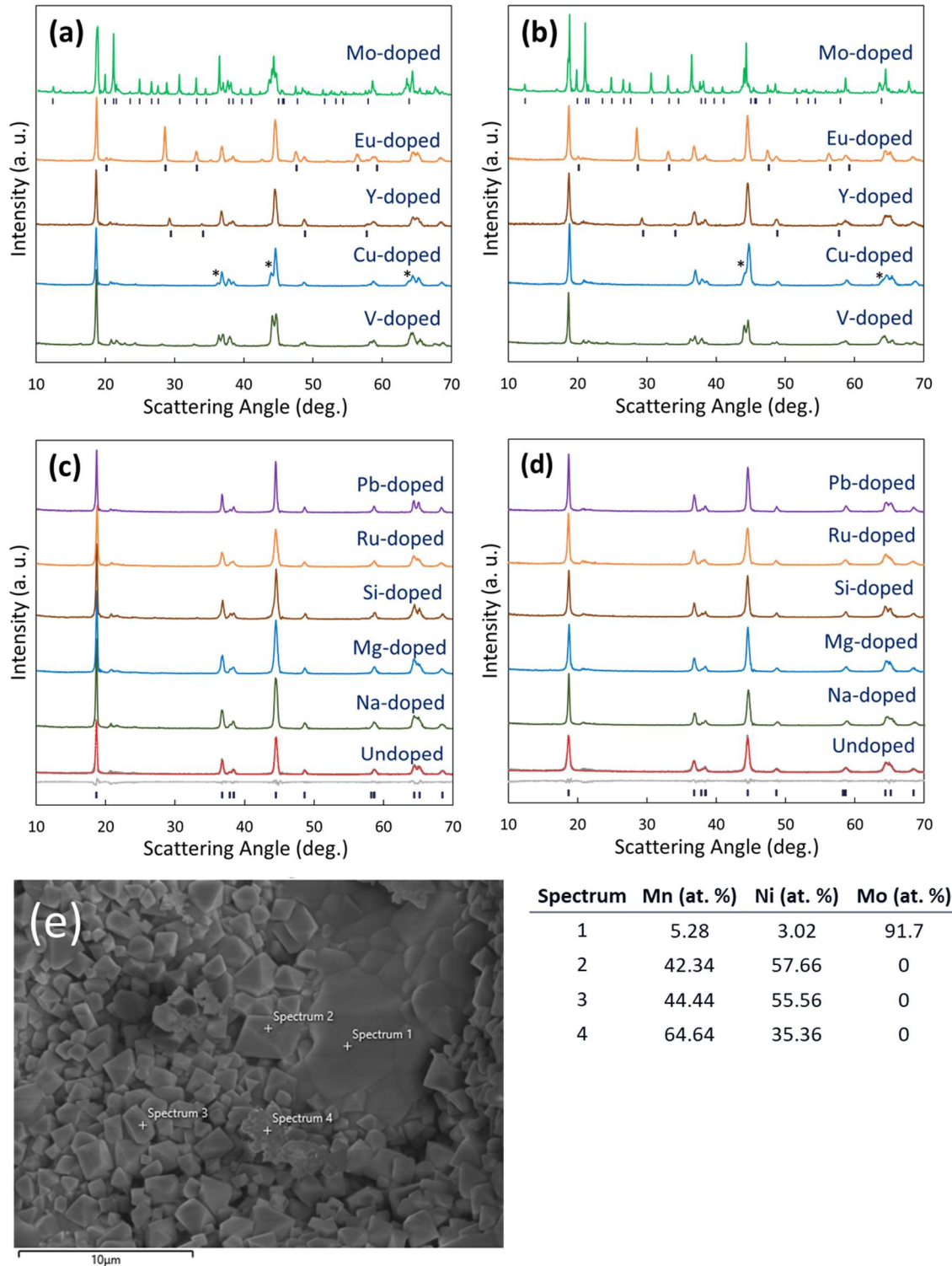


Figure S4. Representative XRD spectra for select multi-phase dopants after sintering at 800 °C (a,c) and 850 °C (b,d). The reference patterns for the Mo-, Eu-, and Y-doped materials correspond to dilithium molybdate, europium oxide, and yttrium oxide respectively. The * refer to peaks from a phase in the undoped Li-Mn-Ni-O phase diagram referred to as the “ordered rocksalt” in ref. ³¹. (e) shows SEM/EDX results for the Mo-doped sample made at 800 °C.

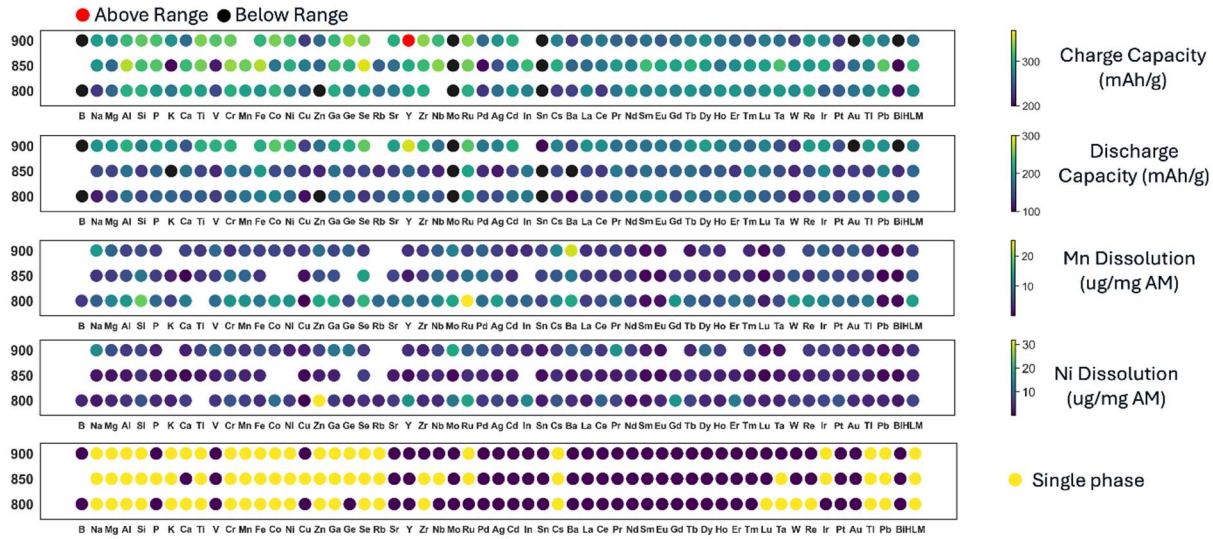


Figure S5. Summary showing how properties change depending on temperature for each dopant.

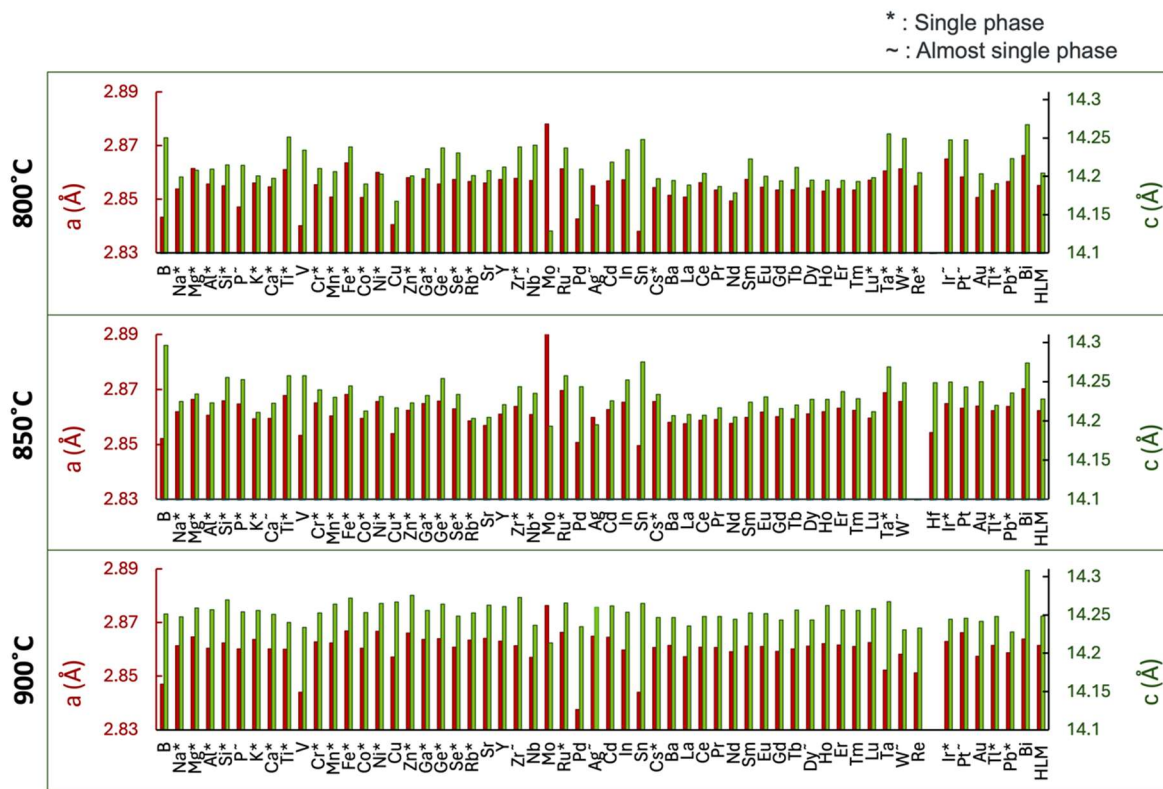


Figure S6. Lattice parameters for doped materials and average of the undoped materials

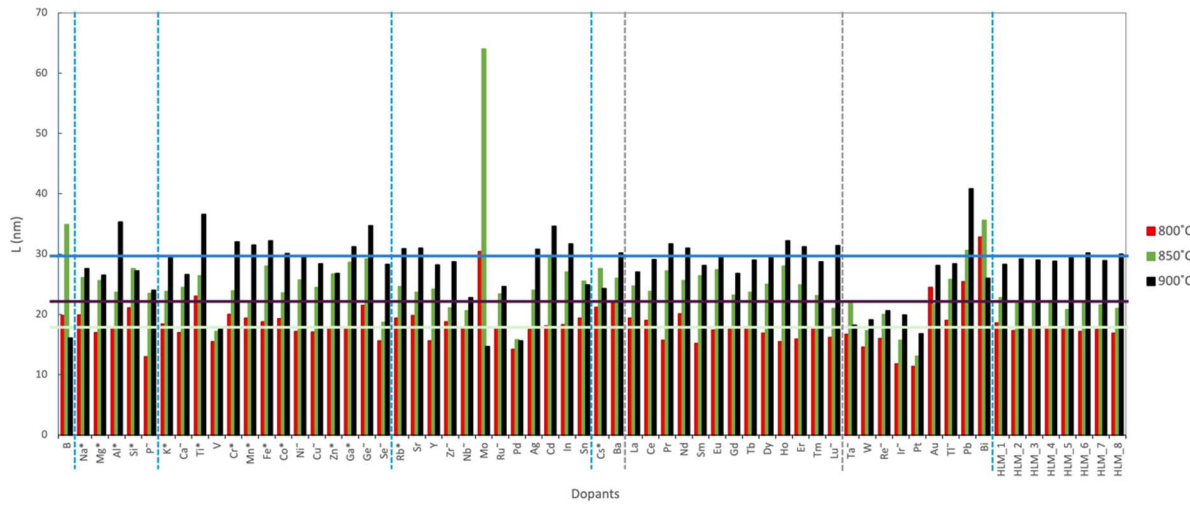


Figure S7. Crystallite size of each dopant at various sintering temperatures.

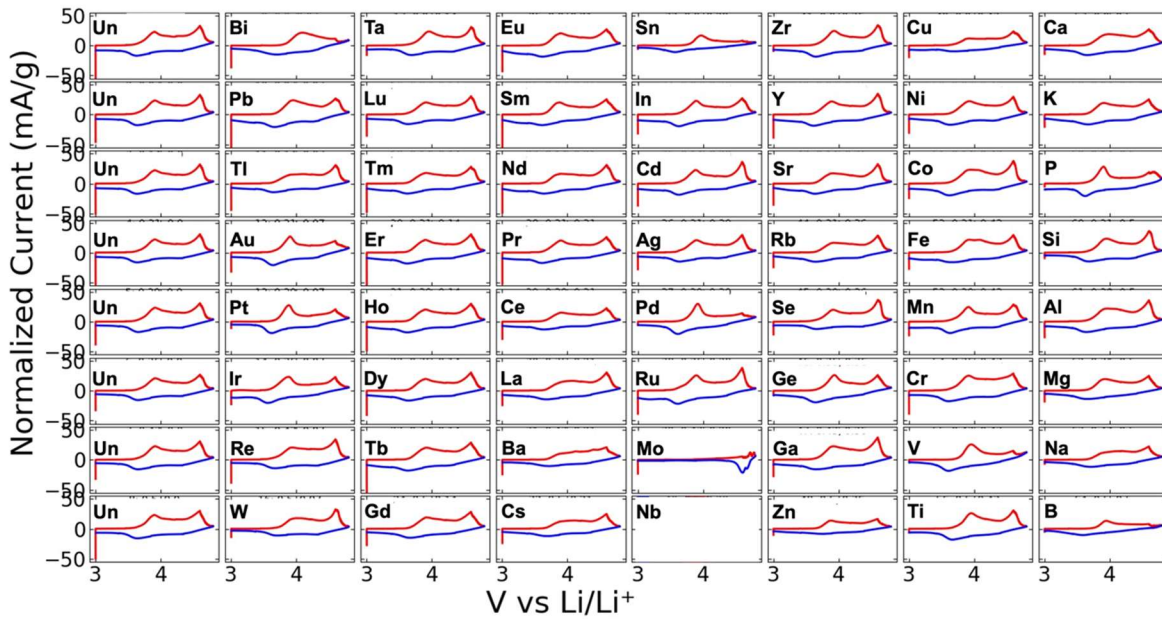


Figure S8. Cyclic Voltammograms of materials sintered at 800 °C.

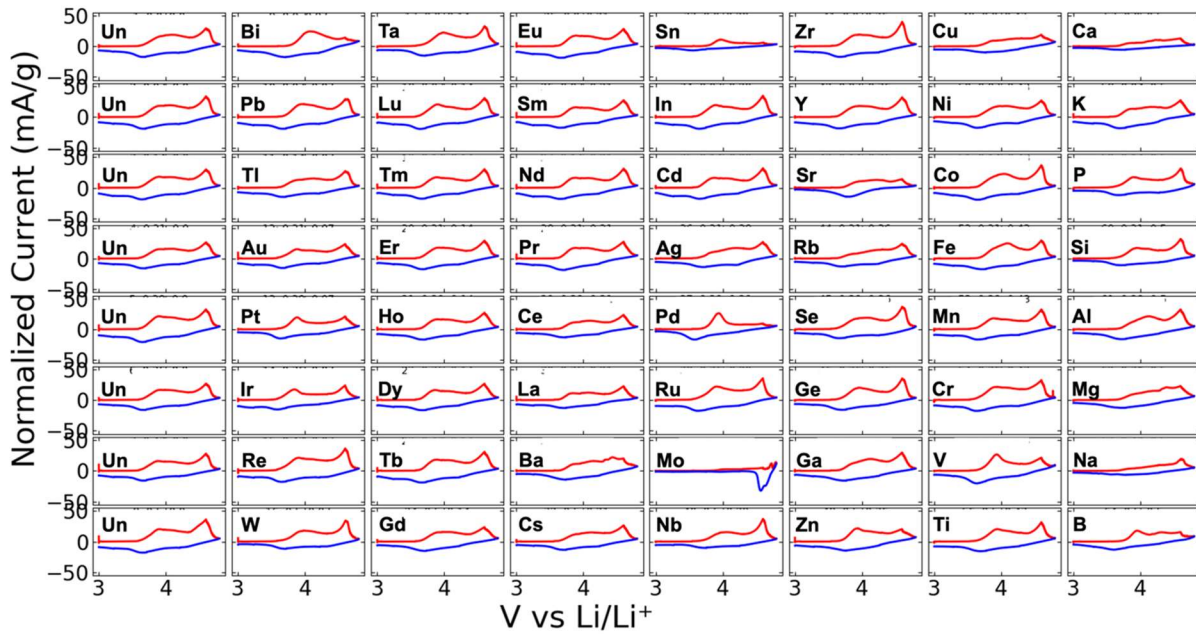


Figure S9. Cyclic Voltammograms of materials sintered at 850 °C.

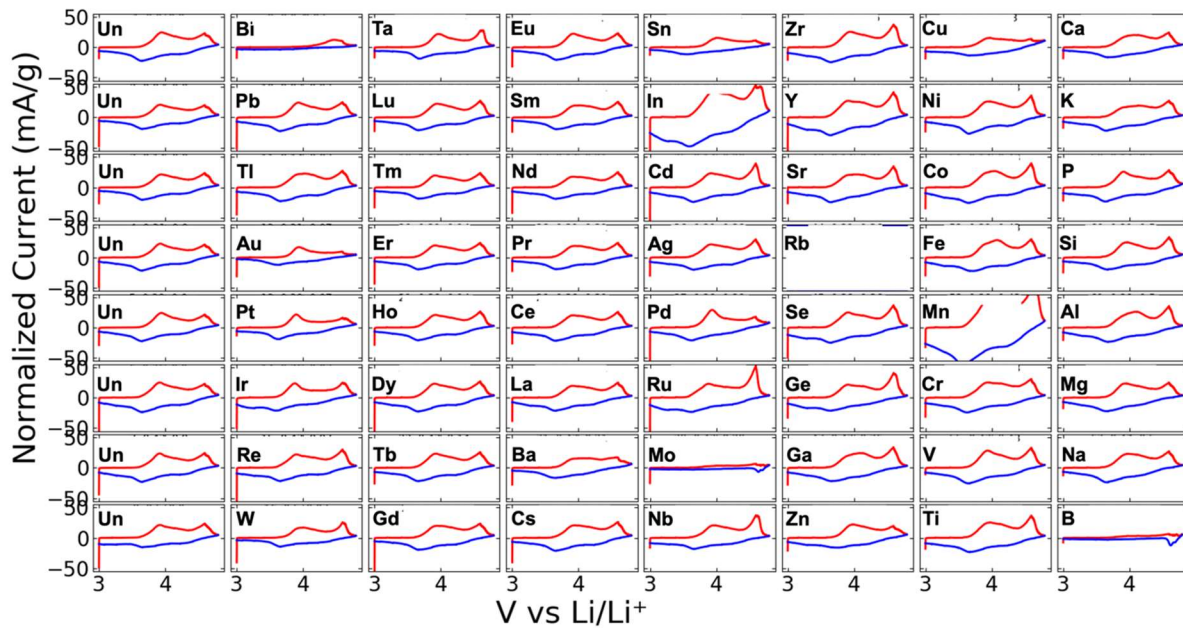


Figure S10. Cyclic Voltammograms of materials sintered at 900 °C.

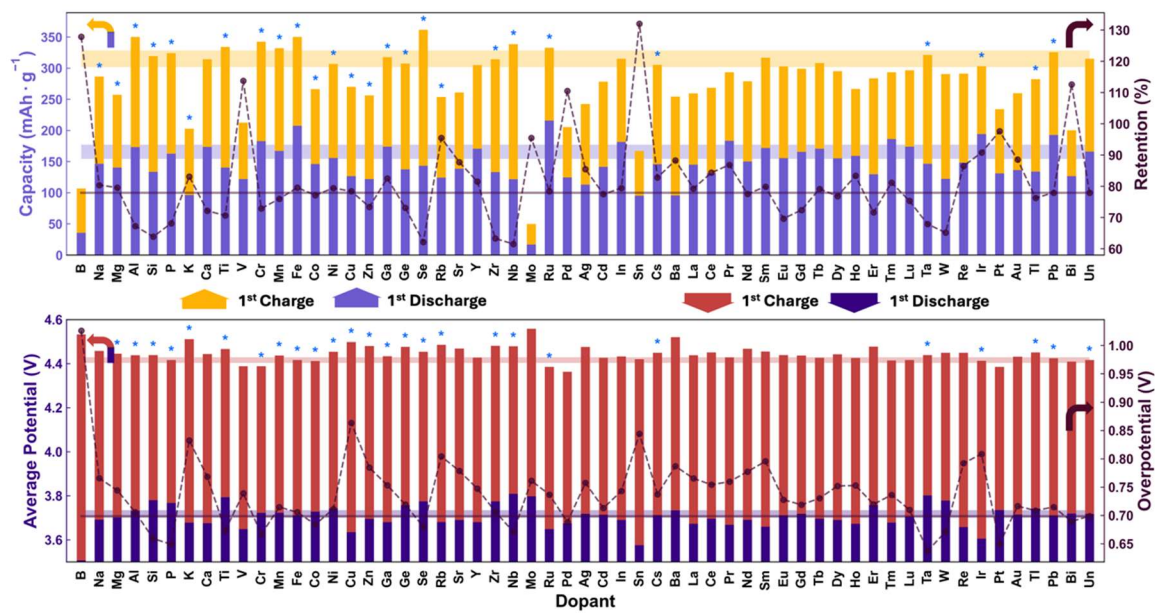


Figure S11. Summary of electrochemistry for materials sintered at 850 °C. (Top) 1st charge and discharge capacities (bars) and retention after 8 cycles (markers). (Bottom) 1st charge and discharge average voltages (bars) and overpotential (markers). Single-phase materials are marked with a *. The translucent bands depict one standard deviation around the mean of eight undoped samples. All data were collected via cyclic voltammetry at a rate of 0.1 V/hr over a potential range of 3 to 4.6 V followed by a rate of 0.02V/hr over 4.6-4.8V on charge and 0.1 V/hr sweet on discharge from 4.8 to 3 V.

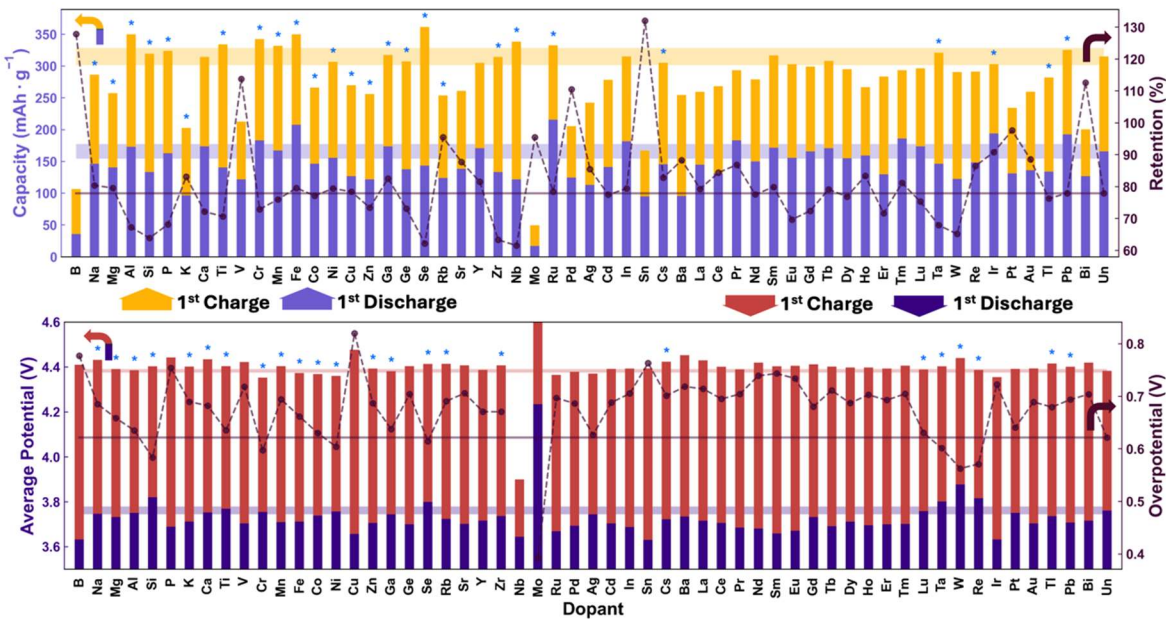


Figure S12. Summary of electrochemistry for materials sintered at 800 °C. (Top) 1st charge and discharge capacities (bars) and retention after 8 cycles (markers). (Bottom) 1st charge and discharge average voltages (bars) and overpotential (markers). Single-phase materials are marked with a *. The translucent bands depict one standard deviation around the mean of eight undoped samples. All data were collected via cyclic voltammetry at a rate of 0.1 V/hr over a potential range of 3 to 4.6 V followed by a rate of 0.02V/hr over 4.6–4.8V on charge and 0.1 V/hr sweet on discharge from 4.8 to 3 V.

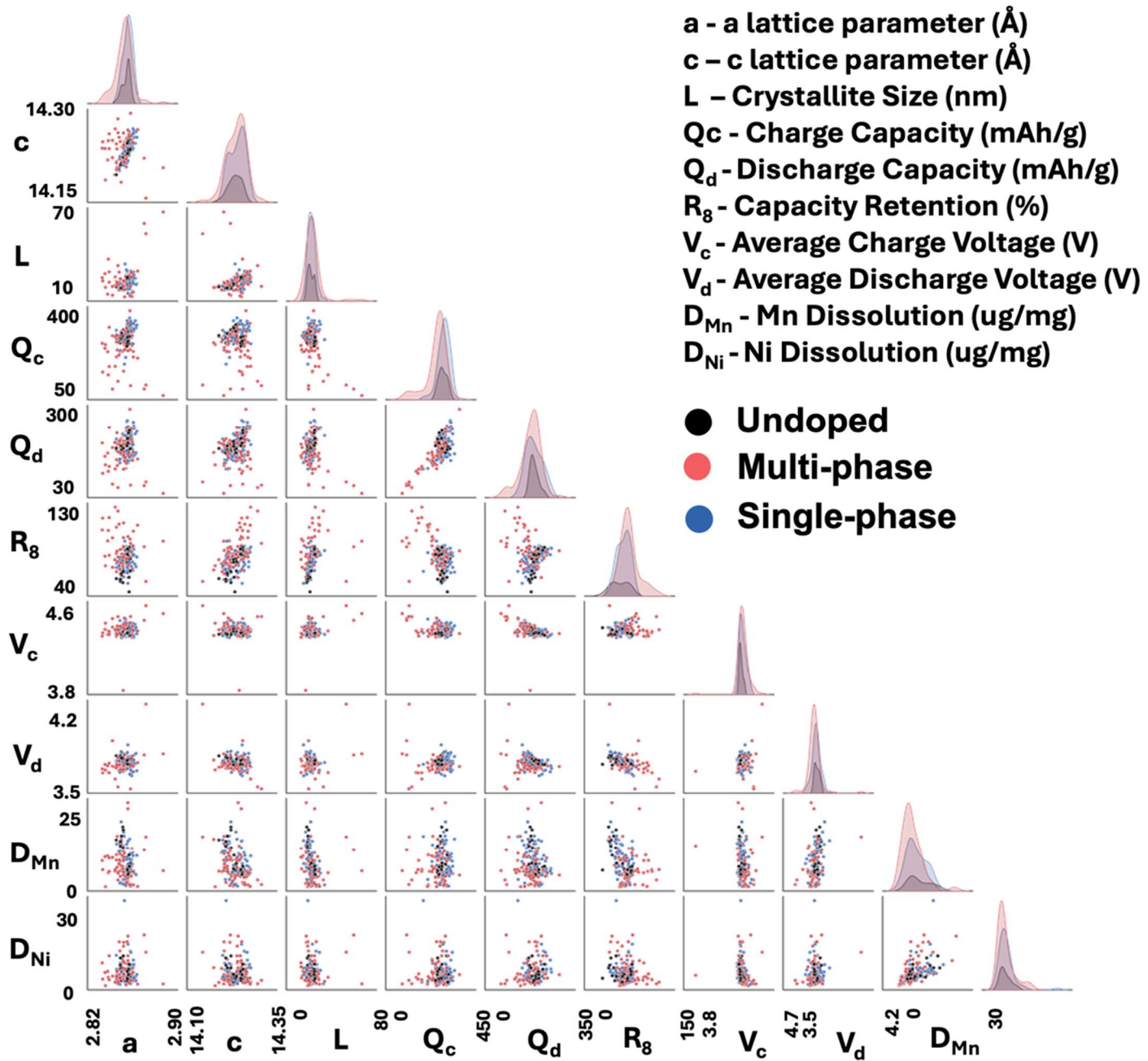


Figure S13. Pair plot of all materials coloured by phase.

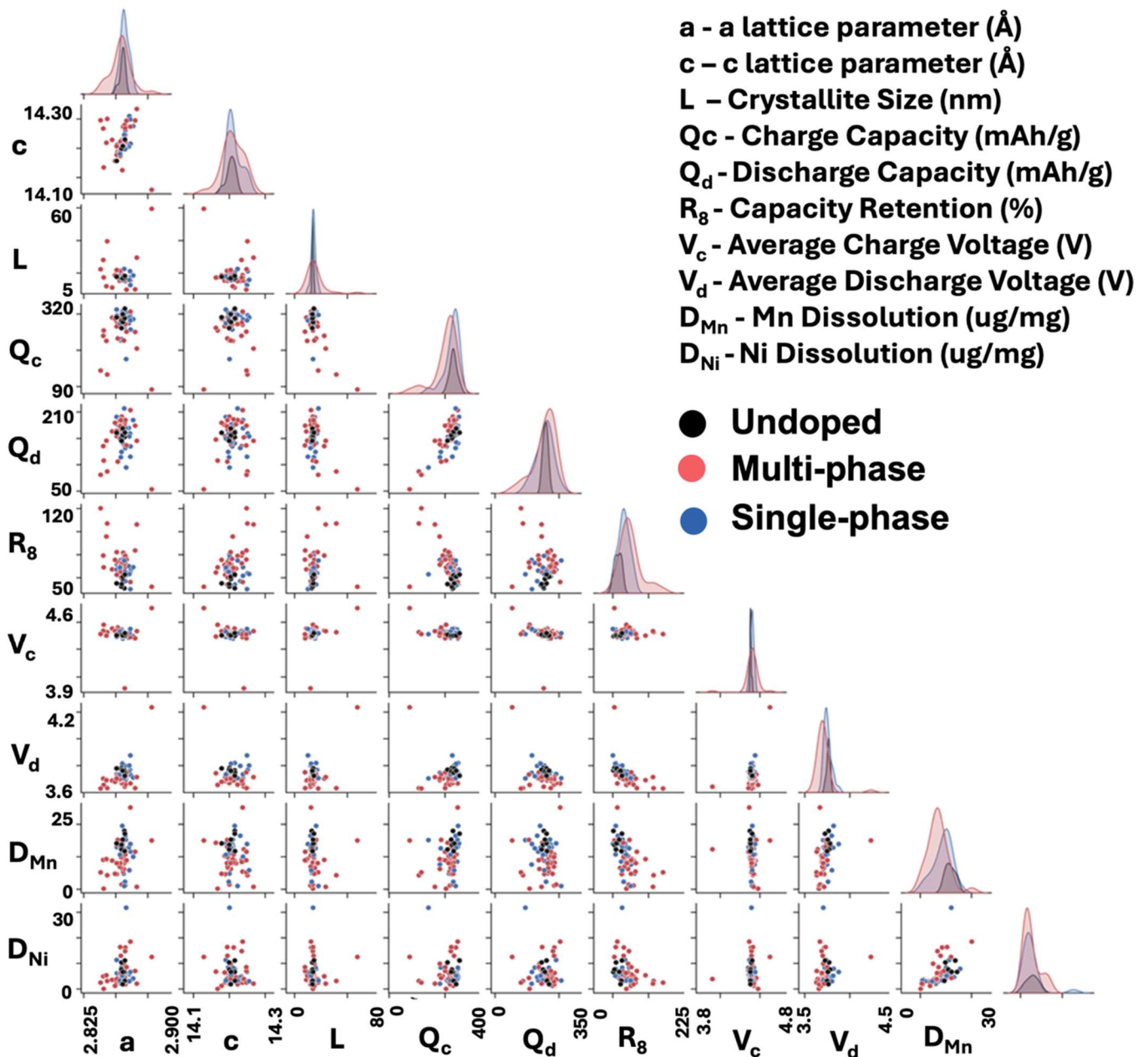


Figure S14. Pair plot of all materials sintered at 800 °C coloured by phase.

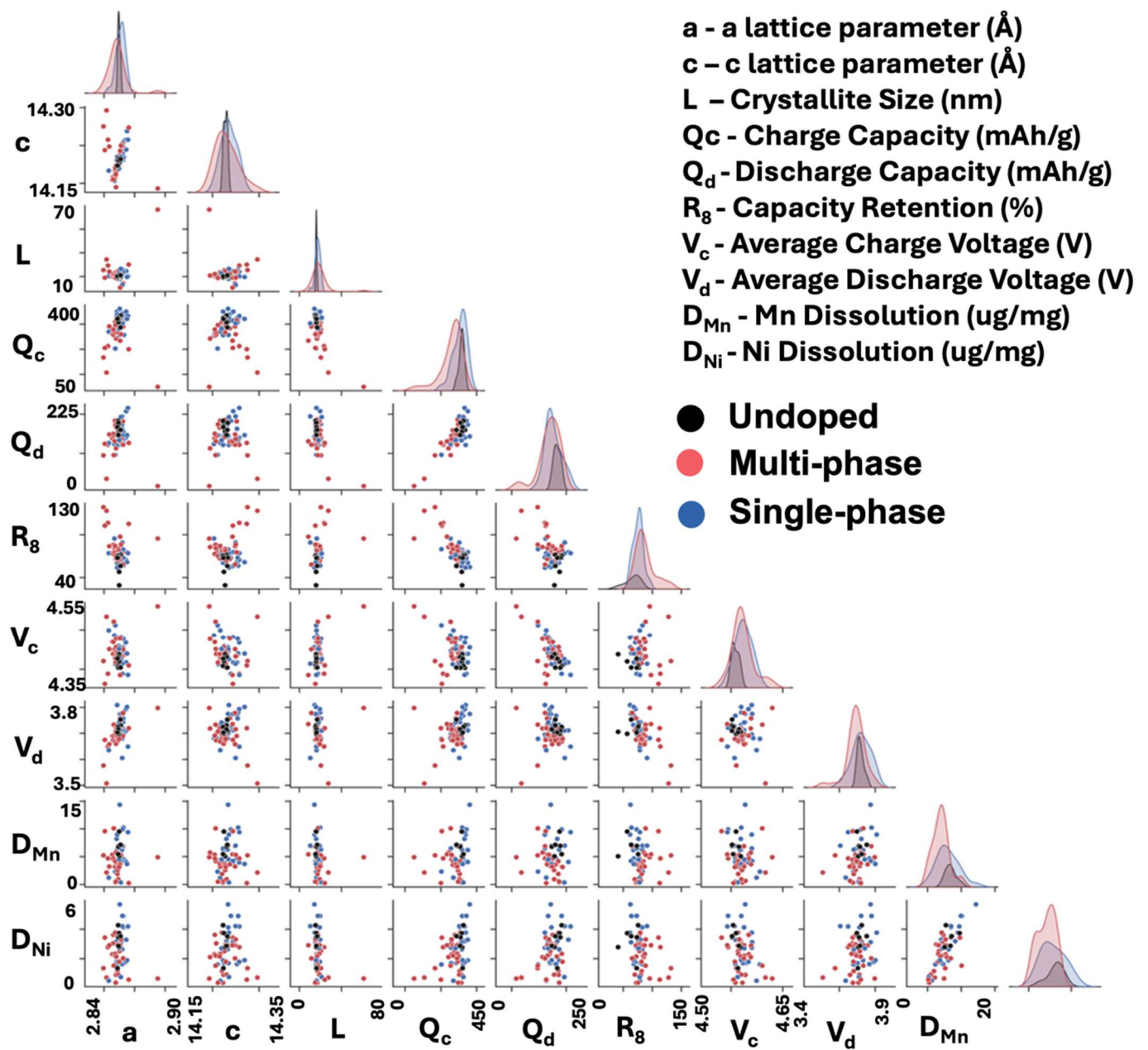


Figure S15. Pair plot of all materials sintered at 850 °C coloured by phase.

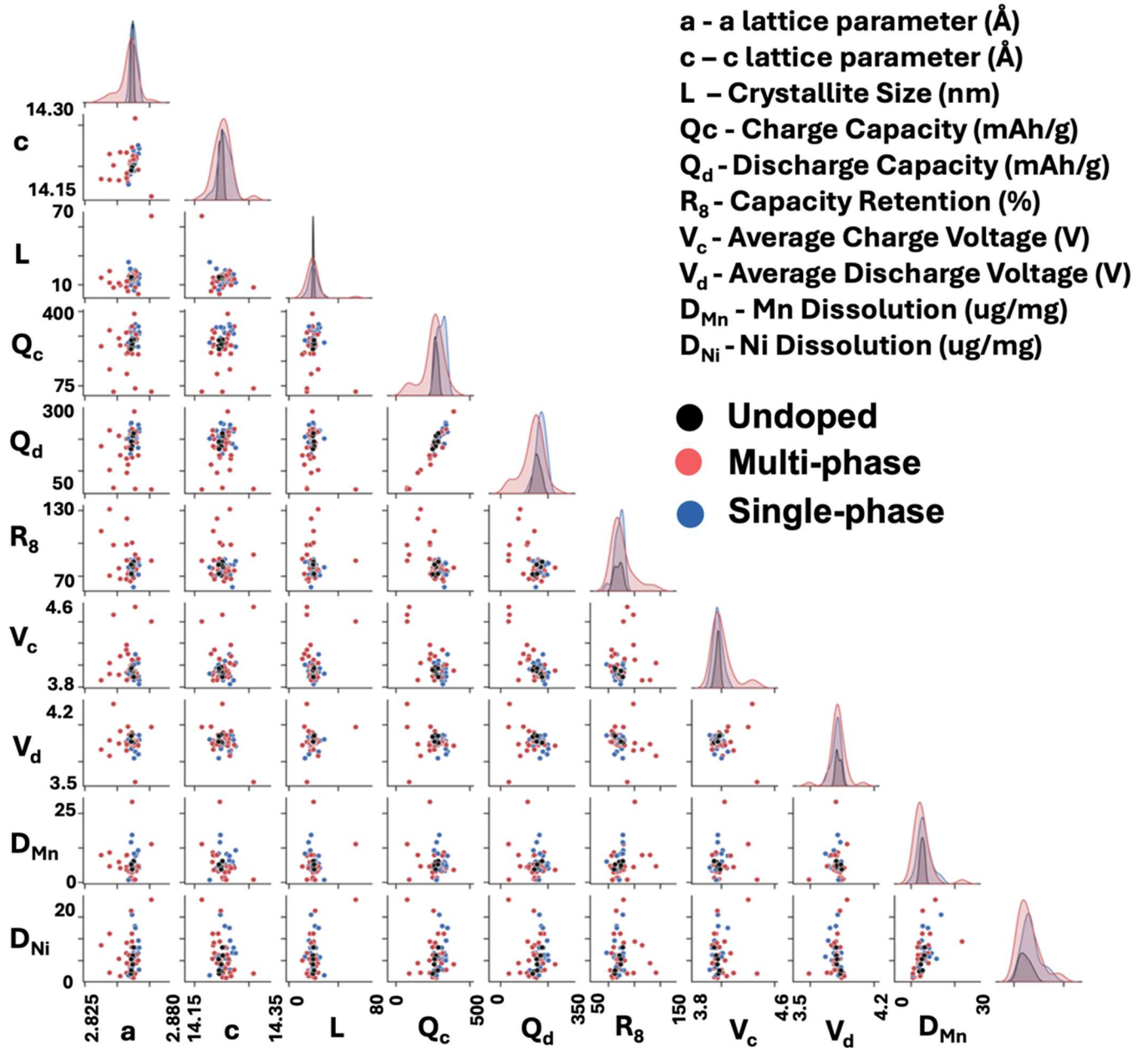


Figure S16. Pair plot of all materials sintered at 900 °C coloured by phase.

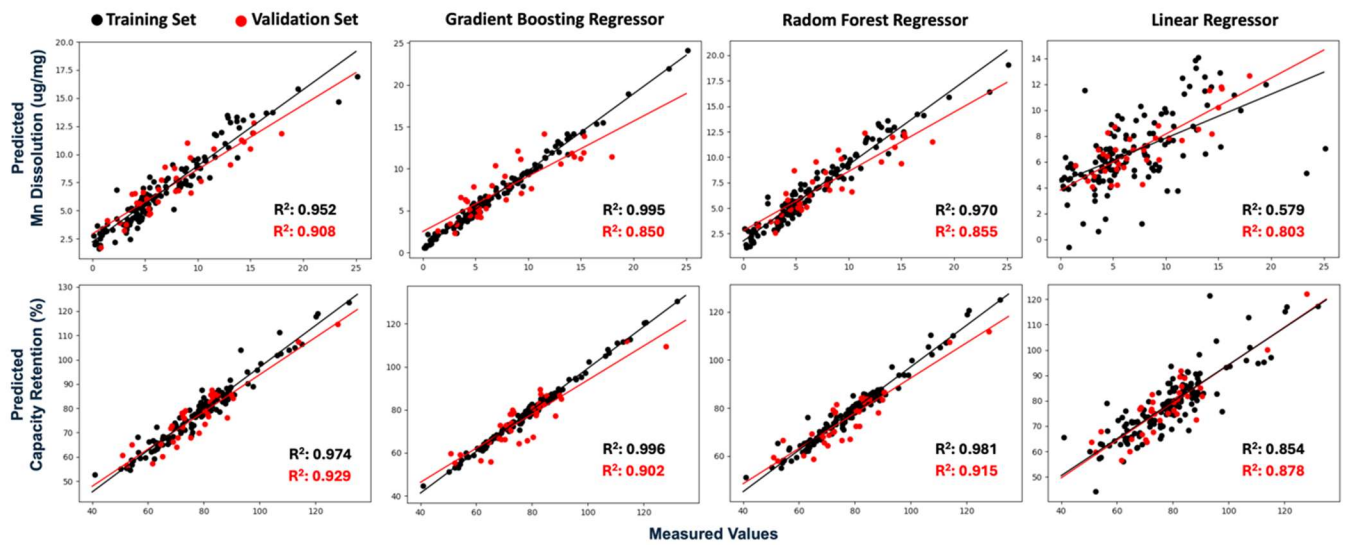
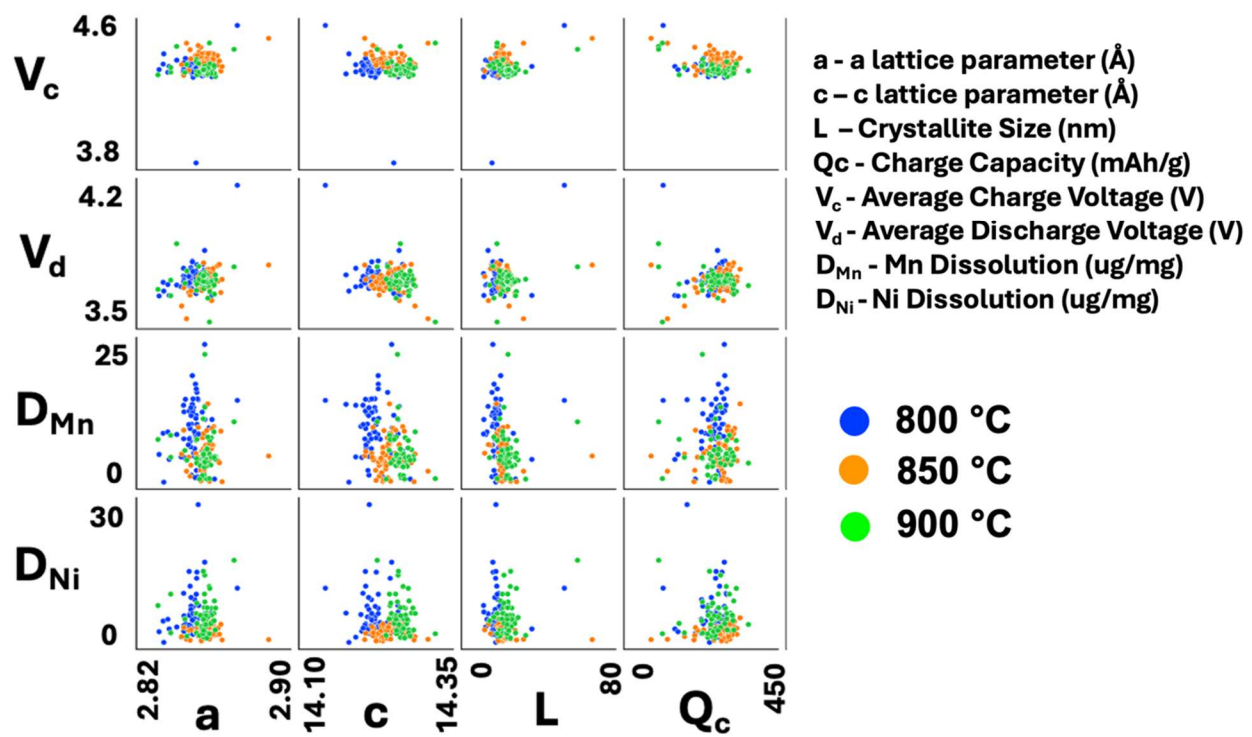
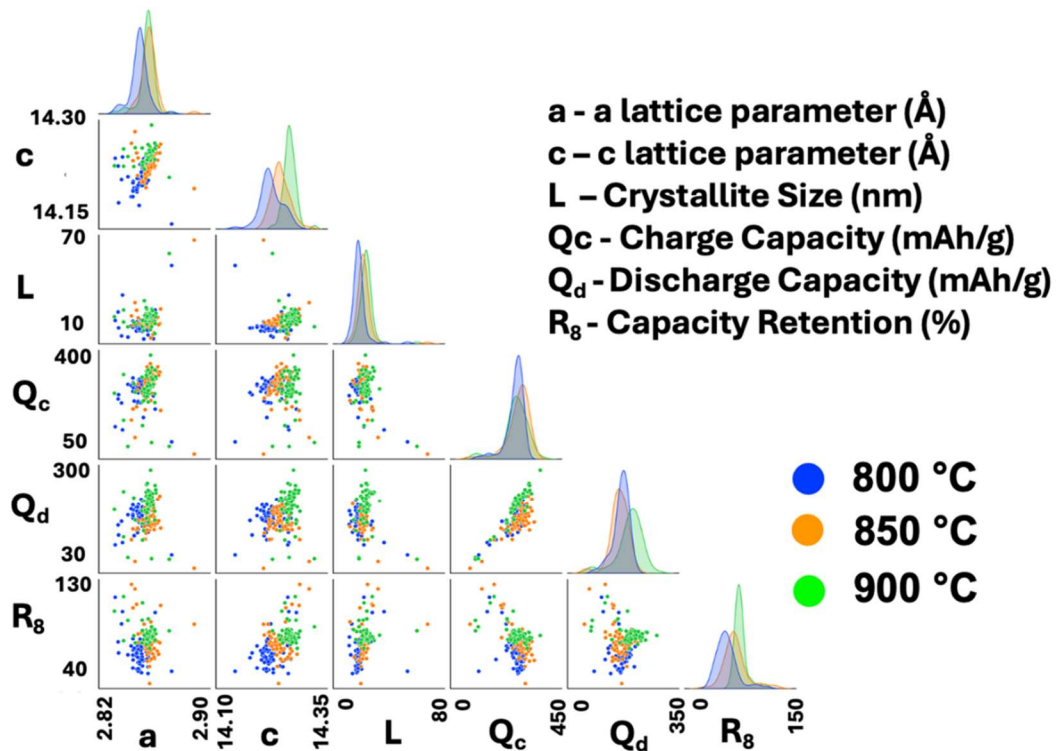


Figure S17. Predicted Mn dissolution (top) and capacity retention after 8 cycles (bottom) for voting model (left) and the components of the voting models with R^2 values for predicting the test set (black) and validation set (red). The left-most are the results from the main text for the voting regressor.



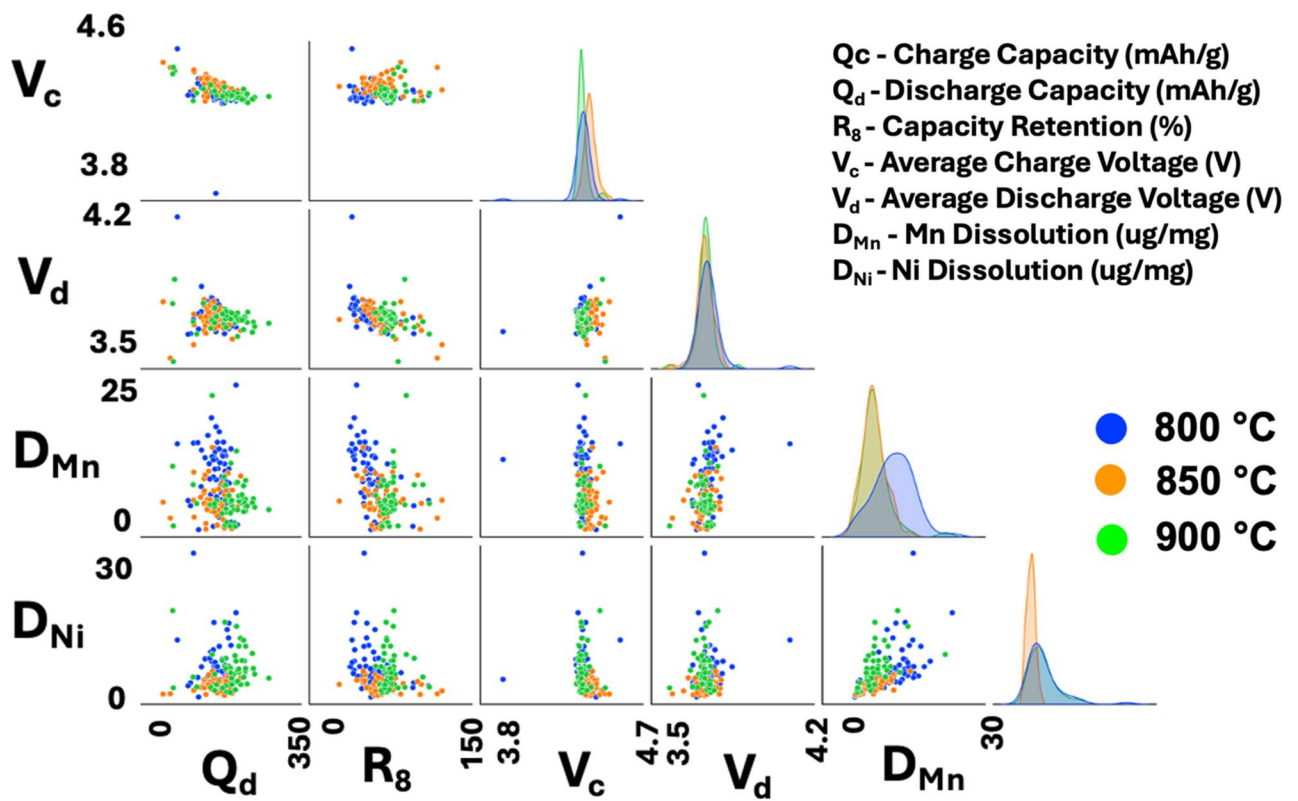


Figure S18. Zoomed in version of Figure 5. Pair plots of cathode properties measured on all 192 materials (both doped and undoped) coloured by sintering temperature. The numbers on the x and y axes represent the minimum and maximum values along the axis.

Machine learning details and interpretation of the random forest model.

The models were trained using data from 168 individual samples. Ten features were used in the training process for predicting Mn dissolution: single phase (boolean), a lattice parameter (A), c lattice parameter (A), cell volume (A^3) grain size (nm), first cycle charge capacity (mAh/g), first cycle discharge capacity (mAh/g), first cycle average charge voltage (V), first cycle average discharge voltage (V), first cycle charge capacity between 4.4 and 4.6 V (mAh/g). The same features were used for training the model to predict discharge capacity retention after 8 cycles. The single phase feature was encoded using one hot encoding and all continuous features were normalized before training. The models were run using scikit-learn library with the parameters in listings S1 and S2.

Looking at the importance of features (a metric that quantifies the magnitude of the contribution from each input) in the random forest model (which gives the second best R² for the test sets behind the voting model) is useful to validate our interpretation of the voting model in the main test. These metrics are shown in Figures S19-S20. This shows that grain size and average voltages are the most important features for TM dissolution. This is certainly consistent with our interpretation of the voting model in the main text where all these features show large changes in the prediction when altered by 1 standard deviation. In the model predicting capacity retention, the random forest model places a large importance on high-voltage charge capacity. This was somewhat captured in our analysis of the voting model where the charge capacity was important. The random forest also placed importance on discharge average voltage and grain size. Both were clearly important in our analysis of the voting model. Thus, looking at the importance of features of the random forest model validates our main conclusions in the main text.

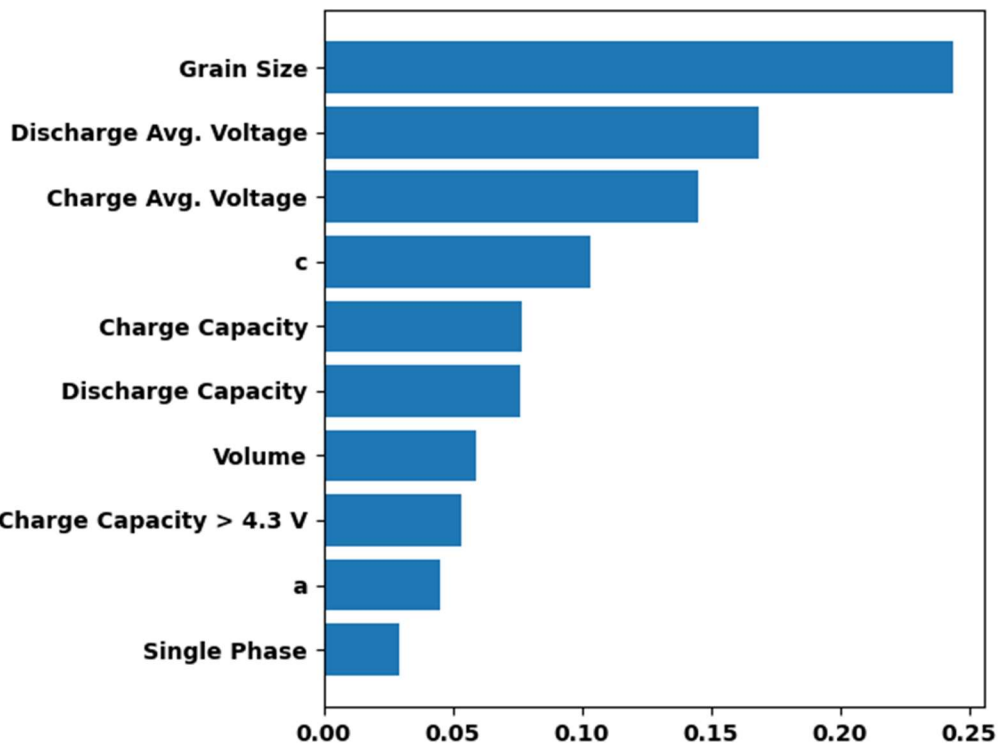


Figure S19. The importance of features for the random forest model for predicting Mn dissolution.

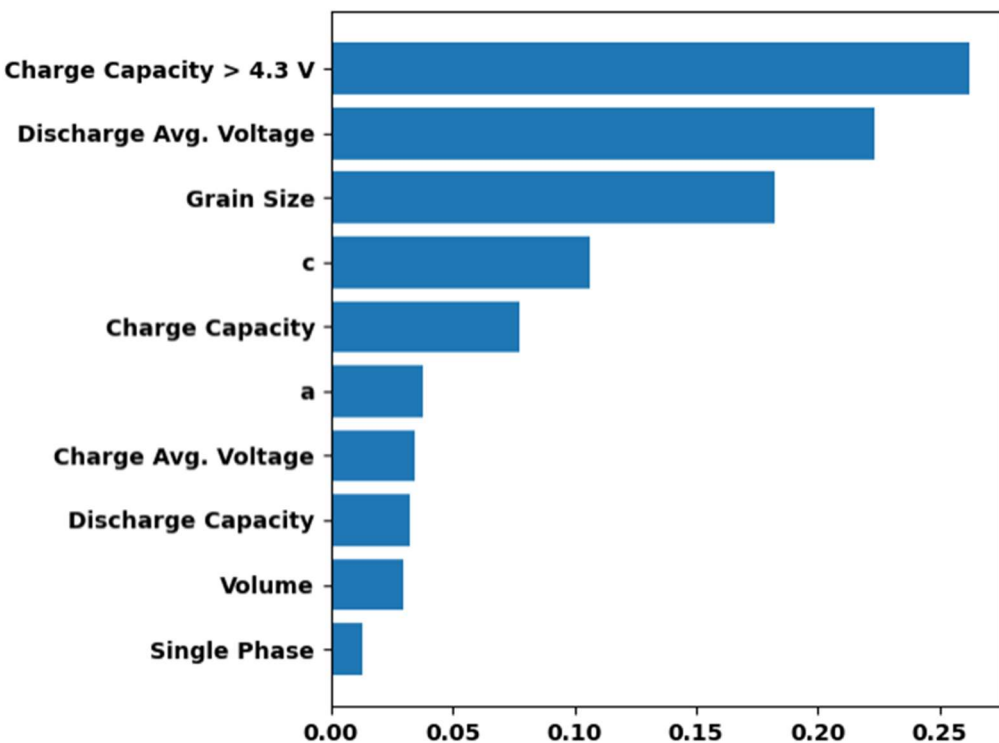


Figure S20. The importance of features for the random forest model for predicting capacity retention.

Listing S1. All parameters from the voting model as outputted by scikit-learn for the voting model for predicting Mn dissolution.

```
{'estimators':  
    [  
        ('gb', GradientBoostingRegressor()),  
        ('rf', RandomForestRegressor()),  
        ('lr', LinearRegression())  
    ],  
    'n_jobs': None,  
    'verbose': False,  
    'weights': None,  
    'gb': GradientBoostingRegressor(),  
    'rf': RandomForestRegressor(),  
    'lr': LinearRegression(),  
  
    'gb_alpha': 0.9,  
    'gb_ccp_alpha': 0.0,  
    'gb_criterion': 'friedman_mse',  
    'gb_init': None,  
    'gb_learning_rate': 0.1,  
    'gb_loss': 'squared_error',  
    'gb_max_depth': 3,  
    'gb_max_features': None,  
    'gb_max_leaf_nodes': None,  
    'gb_min_impurity_decrease': 0.0,  
    'gb_min_samples_leaf': 1,  
    'gb_min_samples_split': 2,  
    'gb_min_weight_fraction_leaf': 0.0,  
    'gb_n_estimators': 100,  
    'gb_n_iter_no_change': None,  
    'gb_random_state': None,  
    'gb_subsample': 1.0, 'gb_tol': 0.0001,  
    'gb_validation_fraction': 0.1,  
    'gb_verbose': 0,  
    'gb_warm_start': False,  
  
    'rf_bootstrap': True,  
    'rf_ccp_alpha': 0.0,  
    'rf_criterion': 'squared_error',  
    'rf_max_depth': None,  
    'rf_max_features': 1.0,  
    'rf_max_leaf_nodes': None,  
    'rf_max_samples': None,  
    'rf_min_impurity_decrease': 0.0,  
    'rf_min_samples_leaf': 1,
```

```
'rf_min_samples_split': 2,  
'rf_min_weight_fraction_leaf': 0.0,  
'rf_monotonic_cst': None,  
'rf_n_estimators': 100,  
'rf_n_jobs': None,  
'rf_oob_score': False,  
'rf_random_state': None,  
'rf_verbose': 0,  
'rf_warm_start': False,  
  
'lr_copy_X': True,  
'lr_fit_intercept': True,  
'lr_n_jobs': None,  
'lr_positive': False  
}
```

Listing S2. All parameters from the voting model as outputted by scikit-learn for the voting model for predicting capacity retention.

```
{'estimators':  
    [  
        ('gb', GradientBoostingRegressor()),  
        ('rf', RandomForestRegressor()),  
        ('lr', LinearRegression())  
    ],  
    'n_jobs': None,  
    'verbose': False,  
    'weights': None,  
    'gb': GradientBoostingRegressor(),  
    'rf': RandomForestRegressor(),  
    'lr': LinearRegression(),  
  
    'gb_alpha': 0.9,  
    'gb ccp_alpha': 0.0,  
    'gb criterion': 'friedman_mse',  
    'gb init': None,  
    'gb learning_rate': 0.1,  
    'gb loss': 'squared_error',  
    'gb max_depth': 3,  
    'gb max_features': None,  
    'gb max_leaf_nodes': None,  
    'gb min_impurity_decrease': 0.0,  
    'gb min_samples_leaf': 1,  
    'gb min_samples_split': 2,  
    'gb min_weight_fraction_leaf': 0.0,  
    'gb n_estimators': 100,  
    'gb n_iter_no_change': None,  
    'gb random_state': None,  
    'gb subsample': 1.0,  
    'gb tol': 0.0001,  
    'gb validation_fraction': 0.1,  
    'gb verbose': 0,  
    'gb warm_start': False,  
  
    'rf bootstrap': True,  
    'rf ccp_alpha': 0.0,  
    'rf criterion': 'squared_error',  
    'rf max_depth': None,  
    'rf max_features': 1.0,  
    'rf max_leaf_nodes': None,  
    'rf max_samples': None,  
    'rf min_impurity_decrease': 0.0,
```

```
'rf_min_samples_leaf': 1,  
'rf_min_samples_split': 2,  
'rf_min_weight_fraction_leaf': 0.0,  
'rf_monotonic_cst': None,  
'rf_n_estimators': 100,  
'rf_n_jobs': None,  
'rf_oob_score': False,  
'rf_random_state': None,  
'rf_verbose': 0,  
'rf_warm_start': False,  
  
'lr_copy_X': True,  
'lr_fit_intercept': True,  
'lr_n_jobs': None,  
'lr_positive': False  
}
```

Table S2: Summary of properties for elements selected from the full dataset (available as its own supplemental file) where both the total TM dissolution and the first discharge capacities are improved compared to the undoped samples at those synthesis temperature. The columns are synthesis temperature (T), dopant used, phase from XRD (1 represents single-phase, 0 represents multi-phase, ~ in the dopant column represents near single-phase), lattice parameters and Scherrer length (L), charge capacity (Ch. Cap.), average charge voltage (Ch. Av. V.), discharge capacity (Dis. Cap.), average discharge voltage (Dis. Av. V.), capacity retention after 8 cycles (% Ret.), Mn dissolution in ug of Mn per mg of cathode (Mn Dis.), Ni dissolution in ug of Ni per mg of cathode (Ni Dis.), and finally a new figure of merit that is the discharge capacity divided by the total TM dissolution in units of mAh per mg of dissolved TM (Dis. Cap./TM).

T (°C)	Dopant	XRD Results (Pristine Material)			Electrochemical Results (3 - 4.8 V)					% Ret.	Mn dis. (ug/mg)	Ni dis. (ug/mg)	Dis. Cap./TM (mAh/mg)
		Phase	a (Å)	c (Å)	L (nm)	Ch. Cap. (mAh/g)	Ch. Av. V. (V)	Dis. Cap. (mAh/g)	Dis. Av. V. (V)				
900	Pb	1	2.8587	14.228	35.7	274	4.38	202	3.72	85.4	0.72		86.3
900	Tb	0	2.8602	14.256	24.1	277	4.37	200	3.73	84.2	1.35	3.22	43.7
900	Tl	1	2.8614	14.248	24	293	4.38	208	3.74	82.3	3.60	3.49	29.3
900	Zr~	0	2.8614	14.273	23.9	340	4.40	232	3.69	83.4	4.25	2.87	32.6
900	Ni	1	2.8668	14.265	24.9	317	4.36	234	3.74	86.7	4.31	2.90	32.4
900	P~	0	2.8601	14.254	19.8	321	4.40	216	3.71	76.9	4.79	2.77	28.6
900	Cd	0	2.8645	14.262	29	308	4.37	223	3.71	84.1	3.27	4.36	29.3
900	Y	0	2.8631	14.261	23.7	391	4.39	288	3.69	85.1	3.62	4.15	37.0
900	Ce	0	2.8609	14.248	24.3	268	4.38	198	3.71	88.2	3.61	5.05	22.8
900	Se	1	2.8608	14.248	24.3	337	4.38	252	3.67	87.8	4.05	5.05	27.6
900	Und*	1	2.8615	14.248	24.563	268	4.39	193	3.72	84.5	5.08	4.42	20.3
850	Ca~	0	2.8594	14.223	21.3	314	4.44	174	3.68	72.1	0.33	0.37	246.8
850	Lu	0	2.8596	14.212	18.8	297	4.42	174	3.71	75.3	0.50	0.38	198.9

850	Pb	1	2.8638	14.235	26.5	326	4.43	193	3.71	78.0	0.35	0.76	173.5
850	Sm	0	2.8599	14.224	23.1	317	4.46	172	3.66	79.9	0.66	0.91	109.6
850	Y	0	2.861	14.221	21.5	305	4.43	171	3.68	81.5	1.89	1.16	55.8
850	In	0	2.8653	14.252	24.2	315	4.43	182	3.69	79.4	2.60	2.30	37.1
850	Tm	0	2.8624	14.228	20.6	293	4.41	186	3.68	81.2	3.14	1.80	37.8
850	Pr	0	2.8591	14.216	23.5	293	4.43	183	3.67	86.9	3.20	2.33	33.2
850	Fe	1	2.8682	14.245	24.6	350	4.42	208	3.71	79.6	4.05	3.29	28.3
850	Tb	0	2.8593	14.22	20.9	308	4.43	171	3.70	79.2	4.20	3.77	21.4
850	Al	1	2.8607	14.223	21.8	350	4.44	173	3.73	67.3	6.20	1.89	21.4
850	Ga	1	2.8649	14.232	25.5	318	4.43	174	3.68	82.5	6.27	2.63	19.5
850	Und*	1	2.8623	14.228	20	315	4.42	166	3.72	65.6	6.83	3.14	16.6
800	Sm	0	2.8574	14.223	15.1	272	4.40	185	3.66	79.0	1.15	1.83	62.1
800	Pb	1	2.8566	14.223	22.6	297	4.40	207	3.71	75.0	0.99	3.29	48.4
800	Eu	0	2.8546	14.2	17.2	285	4.41	191	3.67	72.3	1.44	3.67	37.4
800	Lu	1	2.8571	14.198	16.3	287	4.39	160	3.76	65.2	2.29	3.01	30.1
800	Nd	0	2.8494	14.178	18.7	287	4.42	180	3.68	75.5	4.75	1.22	30.1
800	K	1	2.8561	14.2	16.9	267	4.40	164	3.71	80.3	4.81	2.96	21.1
800	Ge~	0	2.8557	14.237	18.8	270	4.40	169	3.70	81.7	5.42	2.41	21.6
800	Ho	0	2.8531	14.195	15.3	288	4.40	184	3.70	66.3	6.92	2.91	18.7
800	Dy	0	2.8542	14.195	19.2	275	4.40	166	3.71	60.3	6.55	3.74	16.2
800	Au	0	2.8507	14.203	21.9	265	4.39	165	3.70	82.2	8.03	3.87	13.8
800	Tm	0	2.8534	14.193	21.4	275	4.41	173	3.70	69.9	8.01	4.02	14.4
800	Zr	1	2.8578	14.238	17.2	304	4.41	169	3.74	61.7	8.48	3.77	13.8
800	P~	0	2.8471	14.214	11.2	290	4.44	163	3.69	67.3	8.81	3.56	13.2
800	Cd	0	2.8568	14.218	16.9	285	4.39	177	3.70	68.1	7.97	4.59	14.1

800	Fe	1	2.8636	14.238	18.6	286	4.37	185	3.71	69.2	10.00	4.10	13.1
800	Tb	0	2.8537	14.212	17.2	288	4.40	186	3.69	68.5	8.17	6.24	12.9
800	Sr	0	2.8562	14.208	18.2	270	4.41	168	3.70	76.4	9.32	5.65	11.2
800	Ti	1	2.8611	14.251	21.2	296	4.40	159	3.77	64.0	8.00	8.50	9.7
800	Ca	1	2.8546	14.197	16.8	303	4.43	158	3.75	54.0	10.71	5.89	9.5
800	Pr	0	2.8535	14.187	15.4	266	4.39	176	3.68	71.2	10.28	6.44	10.5
800	Al	1	2.8557	14.209	17.9	308	4.39	174	3.75	61.2	13.70	4.75	9.4
800	Ni	1	2.8601	14.203	17.5	274	4.36	170	3.76	70.1	12.87	5.60	9.2
800	Ir [~]	0	2.8651	14.248	10.1	250	4.36	174	3.63	83.7	11.53	7.03	9.4
800	Mn	1	2.8509	14.206	17.9	296	4.40	177	3.71	71.7	12.92	6.14	9.3
800	Ga	1	2.8577	14.21	17.7	305	4.38	172	3.74	63.7	15.30	5.25	8.4
800	Und*	1	2.8551	14.204	17.2	287	4.38	157	3.76	57.2	14.58	6.79	7.4

*Undoped. Values are obtained as the average of 8 replicates.